Cinnamaldehyde Characterization as an Antibacterial Agent towards *E.coli* Metabolic Profile Using 96-blade Solid Phase Microextraction Coupled to Liquid Chromatography-Mass Spectrometry

Fatemeh Mousavi[1], Barbara Bojko[1,2], Vincent Bessonneau[1], and Janusz Pawliszyn*

1) Department of Chemistry, University of Waterloo, 200 University Avenue West, Waterloo, Ontario N2L 3G1, Canada
2) Department of Pharmacodynamics and Molecular Pharmacology, Faculty of Pharmacy, Collegium Medicum in Bydgoszcz, Nicolaus Copernicus University in Toruń, Poland

Corresponding Author

Tel.: +1-519-888-4641; Fax: +1-519-746-0435. E-mail: janusz@uwaterloo.ca

ABSTRACT

Sampling and sample preparation plays an important role in untargeted analysis as it influences final composition of the analyzed extract and consequently reflection of the metabolome. In the current work, mechanism of bactericidal action of cinnamaldehyde (CA) against *Escherichia coli* (*E.coli)* during bacteria growth applying high throughput solid phase microextraction (SPME) in direct immersion mode coupled to high performance liquid chromatography-mass spectrometry (HPLC-MS) system was investigated. Numerous discriminant metabolites due to CA addition to the bacteria culture were mapped in the *E.coli* metabolic pathways. We propose new metabolic pathways confirming that CA acts as an oxidative stress agent against *E.coli*. The results of the current research have successfully demonstrated that CA changes the bacterial metabolism through interactions with different biochemical families such as proteins, nucleic acids, lipids, and carbohydrates, which needs further validation by proteomics and transcriptomics studies. The results presented here show great potential of the novel approach in drug discovery, and food safety.

KEYWORDS: metabolomics, sample preparation, SPME, LC/MS, antibacterial agent

1. INTRODUCTION

In recent times, transcriptomics, proteomics, and metabolomics, as functional genomics techniques, have burgeoned investigative fields in different areas of research; however, their challenging methodologies, particularly for in vivo analysis, have abated further progress in various areas of research.[1] Metabolites are the building blocks of proteins, RNA, DNA, and cell membranes. They play important roles in system metabolism, signaling, and regulation with provision of vital components for life.[2,3] The goal of metabolomics is to generate the metabolic profiles of biological systems at a specified time and under specific environmental conditions. As metabolomics has the closest proximity to the phenotype of a given biological system, any environmental perturbation in a given biological system is reflected rapidly in its metabolome. Also, in comparison to other 'omics' approaches, the high-throughput approach available for metabolic analyses of large numbers of samples provides a more cost effective alternative for determinations of changes in biological systems.[4]

Recently, microbial metabolomics has received a lot of scientific attention due to its potential applications in a wide range of research areas, for instance metabolic engineering, and drug discovery and development.[5] Biofilm formation on food as well as exposure of food contact surfaces to human pathogens enhances their ability to survive in harsh environments, as well as their resistance in response to antibacterial treatments. In this regard, one of the most important areas of research in microbial metabolomics involves investigations into the bactericidal modes of action of antibacterial agents against different bacterial strains.[6]

Plants, as a rich source of biologically active components, have been prominently used as a basis for drug development, contributing to human health.[7] Essential oils, as secondary products of aromatic plants, are mixture of volatile compounds that are characterized by a strong odor, and used as food preservers due to their antiseptic, bactericidal, virucidal, fungicidal, and medicinal properties. The cytotoxic nature of these compounds is attributed to the presence of phenol,

aldehyde, and alcohol functional groups in their structures, which have a pro-oxidant effect on proteins and DNA through the generation of reactive oxygen species.[8-14]

Cinnamon is one of the oldest herbal medicines used as a spice and traditional medicine. Cinnamaldehde (CA), as the main component of cinnamon bark extract, produces its distinct cinnamon odor and flavor. This compound has been proven to be active against pathogenic bacteria, fungi, and viruses.[15,16,17] The target action of cinnamon is introduced either on cell structure and membrane functionality, proteins and enzymes, or other essential processes involved in biosynthesis or energy generation.[11] CA is also capable of altering the lipid profile of the microbial cell membrane.[18] Consequently, tracking biochemical alterations during treatment of the biological system by this antibacterial agent could be used to find specific biomarkers or pathway mechanisms.

Metabolomics has been conducted through the use of a variety of analytical platforms, although MS coupled to LC or GC has been most regularly applied. The most important goal in untargeted analysis is to detect as many metabolites as possible so as to enhance the chances of detecting dysregulated metabolites in a biological system, which can indicate the metabolic pathways affected by the stimuli.[19] Due to the complexity of the biological matrix under study, in this case, bacteria media, appropriate sample preparation steps need to be taken prior to analysis so as to reduce possible matrix effects.[4] To this extent, different sample preparation techniques have been introduced for bacterial metabolomics, each with its own set of advantages and disadvantages. In recent times, SPME has been successfully shown as a feasible technique for global metabolomics determinations.[20,21] The use of SPME towards metabolomics applications includes several advantages, such as its applicability for in vivo analysis, reduced matrix effects, extraction of a wide variety of metabolites, extraction of unstable or short-lived metabolites, circumvention of chemical modification, and contamination probable in solvent-based extraction techniques.[21,22]

Recently, qualitative and semi-quantitative analyses of metabolic responses of *E.coli* to CA were conducted through the use of headspace SPME coupled to GC-MS (HS-SPME-GC-MS). This

research showed that the metabolic profile of *E.coli* treated by CA changed in comparison to control samples. In this research, 25 volatile and semivolatile metabolites were identified in the HS of complex biological samples.[23] The current research presents a comprehensive study of *E.coli* bacteria affected by CA, performed with the recently developed SPME-LC/MS protocol to evaluate potential biomarkers related to the microorganism's response to stress induced by the biologically active component.[24] The developed 96-blade SPME-HPLC-MS method provides a comprehensive as well as unbiased metabolic profile, ranging from polar metabolites such as amino acids and nucleotides, to nonpolar metabolites such as lipids. The method is simple, fast, reproducible, and incorporates a metabolism-quenching step while providing high-throughput analysis. With the proposed protocol, the extraction of both hydrophilic and hydrophobic metabolites can be performed in one experiment, making this method a time-efficient alternative as compared to solvent-based sample preparation methods. For this series of experiments, The HPLC method coupled to Orbitrap mass spectrometer with high mass resolution, excellent analytical sensitivity, signal stability, and mass accuracy was applied for comparative global metabolomics profiling.

The optimized protocol was applied to sets of samples of *E.coli* harvested at different growth phase time points. The samples were treated with CA at concentrations ranging from lower to higher than minimum inhibitory concentration (MIC). Different trends in metabolite concentrations were observed over time for each set of experiments, and multivariate analysis was applied towards determinations of statistically significant discriminating features between control and test groups. The observed changes reflected perturbations in the regular metabolic pathways of *E.coli* induced by the bactericidal effect of CA. The findings were supported by results previously obtained from transcriptomics and proteomics studies while there are also some new findings reported in current study.

2. MATERIAL AND METHODS

2.1. Chemical and Materials

LC-MS grade solvents and LC-MS grade formic acid (1 mL glass ampules) were obtained from Fisher Scientific (Ottawa, Canada). Polypropylenes deep 96-well plates (Nunc) and easily modified polystyrene–divinylbenzene (Macherey-Nagel) particles were purchased from VWR International (Mississauga, Canada). All metabolites, peptone, yeast extract, NaCl, and CA were purchased from Sigma–Aldrich. *E.coli* BL21 samples were donated from the laboratory of Professor John Brennan at McMaster University (Hamilton, Ontario, Canada). The Concept 96-SPME-blade unit and robotic Concept 96 autosampler were purchased from Professional Analytical Systems (PAS) Technology (Magdala, Germany) for SPME sample preparation.

2.2. Bacterial Strain, Culture Condition, and CA Effect on Bacterial Strain Growth

E.coli BL21 was used as non-pathogenic bacteria for the currently presented microbial metabolomics study. Standard Luria Bertani (LB) media (10 g trypton, 5 g yeast extract, and 5 g NaCl in 1 L nanopure water) was used as media for growth of bacteria, while LB agar media (10 g trypton, 5 g yeast extract, and 5 g NaCl; 15 g Agar in 1 L nanopure water) was used to count the number of colonies forming in units per mL (CFU mL^{-1}) in bacterial suspensions. Cells were grown in nutrient media at 37°C and 125 rpm for 24 hours. To provide countable numbers of colonies present in agar media, cultures were serially diluted with sterile media. Next, 100 µL of diluted media were distributed on the warm agar plate, and incubated at 37°C for a 24-hour period. The growth curve of *E.coli* culture was obtained by counting the CFU mL^{-1} from the first moment of bacteria addition to LB media up until 24 hours had elapsed.

The antibacterial activity was determined by an agar dilution method (according to the guidelines of Clinical and Laboratory Standard Institute). Different concentrations of CA in methanol (0-2000 mg L^{-1}) were added into the 96-well plate containing a suspension of bacterial cells with an initial concentration of 10^5 CFU mL^{-1}. Subsequently, growth curves were obtained for each of

the *E.coli* cultures. Final and initial CFU mL^{-1} figures were obtained for control cultures and CA-treated cultures grown under the same conditions, and used to obtain a MIC value for CA.

2.3. Metabolite Extraction and Metabolic Profiling Using 96-blade-SPME-UPLC-MS

In the present study, for each set of samples, bacteria were cultivated in sterile 96-well plates. Subsequently, the 96-thin film (blades) SPME system operated by the robotic Concept 96- was applied for in vivo metabolite extractions. The stainless steel blades were coated with PS-DVB-WAX:HLB 50:50 [w/w]. The coating preparation procedure as well as information related to the concept autosampler have been reported in previous works.[24,25] Different types of experiments were designed in order to evaluate results in terms of different errors (biological or nonbiological) and explain significant biological differences with higher confidence. Biological replicates were obtained to differentiate between random results and statistically significant differences between two groups of samples exposed to different treatments, so as to ascertain whether the observed differences represent a true biological difference induced due to treatment with the naturally-occurring antibacterial agent.

The experimental design consisted of two approaches: in the first case, bacteria was treated with CA (below and above MIC) at the beginning of incubation, and extraction was performed at 0, 3, 6, 9, 12, and 15 hours from 1 mL of *E.coli* culture in sterile LB media (initial concentration 5.0 log CFU mL^{-1}). As a control, a sample obtained from the same batch of *E.coli* culture was extracted under identical conditions with no CA addition. In the second case, CA (above minimum inhibitory concentration) was added every three hours after *E.coli* incubation up to the 15th hour. For each time point, metabolic profiling data was obtained in triplicate.

The SPME procedure conditions for all experiments were as follows: coatings were conditioned for 120 min in 1 mL ethanol:water 70:30 (v/v) mixture in the 96-well plate with orbital agitation set at 850 rpm. Next, extraction from 1 mL 5.0 log CFU mL^{-1} *E.coli* (initial concentration) in

8

sterile LB media was carried out in direct immersion mode for 60 min with agitation speed set at 1000 rpm (2.5 mm amplitude). After extraction, coatings were washed for 30 seconds in 1 mL of distilled water with 0.1% formic acid under agitation at 850 rpm in order to remove loosely attached particulates and salt from the surface of the sorbent. Desorption was performed in 1 mL acetonitrile:water 50:50 (v/v), at 1500 rpm speed for 60 min. Next, the desorption solution was transferred to the autosampler of the LC–MS system for separation and quantitation. Optimization of the SPME protocol is described in previous study.[24]

Chromatographic separation was performed with a Kinetex PFP column [100 × 2.1mm, 1.7μm] (Phenomenex, Torrance, CA, USA) with a guard filter (Security Guard ULTRA Cartridges UHPLC PFP for 2.1 mm). The column temperature was maintained at 25°C, and gradient mobile phase conditions were composed of phase A (water containing 0.1% formic acid) and phase B (acetonitrile with 0.1% formic acid) with the following set conditions: 0-1 min 90% A; 1-9 min 90-10% A; 9-12 min 10% A; 12-16 min 10-90% A. All extracts were injected randomly, while blank and Pooled quality control (QC) samples were analyzed following introduction of every set of 15 samples throughout the sequence as to avoid cross contamination, as well as verify instrument performance. The QC sample was prepared by mixing 10 μL aliquots of each extract. The injection volume was 10 μL. Autosampler temperature was set at 4°C, and extracts were kept at 4°C.

The high-resolution orbitrap Exactive mass spectrometer (Thermo, San Jose, California, USA) was operated in both negative and positive electrospray ionization (ESI) modes and at 50-1000 m/z mass range. Optimum sheath gas (arbitrary units), auxiliary gas (arbitrary units), ESI voltage (kV), capillary voltage (V), capillary temperature (°C), and tube lens voltage (V) were set at 40, 25, 4.0, 27.5, 275, and 100 for positive ESI mode, and 50, 25, -2.7, -67.5, 325, and -85 for negative ESI mode. External instrument mass calibration was performed every 24 h, resulting in 2 ppm mass accuracy. Compound identification was confirmed for discriminant features using a Q-Exactive mass spectrometer (Thermo Fisher Scientific, CA, USA) operating in positive and

negative ionization modes with the same chromatographic conditions as the primary analysis. Collision energy ranging from 50-100 V was applied for MS/MS fragmentation of target ions.

2.4. Metabolite Identification, Data Mining, and Statistical Analysis

The raw data (.raw) obtained with Xcalibur software version 2.1 (Thermo) was converted to (mzXML) with the MS conversion software. The converted data was then processed with the XCMS R-package (Scripps Center for Metabolomics, California, USA). The output is a table containing retention times, m/z, and intensity of features.[20] Alignment, framing, peak picking, and feature detection were done with R software. The CAMERA R-package (Bioconductor Version 2.10) was applied to provide ion annotation on the list of features so as to identify detected isotopes, adducts, and in-source fragment ions.

Putative identification of discriminant compounds was based on comparisons of their accurate masses with METLIN online database queries, using a 5 ppm tolerance window. Data from MS/MS METLIN and MassBank databases as well as literature surveys were subsequently applied to confirm the identification of putative candidates. Moreover, commercially available chemical standards were analyzed by LC-MS and LC-MS/MS to confirm metabolite identities of the most significant metabolites by retention time and mass spectral matching. Ions were targeted by collision energy and the MS/MS fragmentation pattern and retention time of discriminant features were compared by those of commercially available chemical standards.

Multivariate data analysis was performed with the use of SIMCA-P+ software (Umetrics, NJ, USA) for statistical analyses. The Principal Component Analysis (PCA) was used to assess the quality of data and Partial Least Squares-Discriminant Analysis (PLS-DA) was applied to assess information regarding variances in metabolic phenotypes corresponding to bacteria cultures treated with antibacterial agents at different time points in comparison to control samples at the same time intervals. All processed data of each chromatogram were normalized and Pareto scaled, prior to multivariate statistical analysis. Statistically significant variables between treated *E.coli* by CA and control *E.coli* cultures were acquired by analysis of S-plots obtained from

10

OPLS-DA score plots. The KEGG database was used in the identification of important metabolic pathways and subsequent biological interpretations. For this data processing step, abundant dysregulated features were filtered according to the following criteria: p-value < 0.01, fold change >1.5, and MS peak intensity >10000 ion counts, representing the threshold required to generate high-quality MS spectra on an Orbitrap instrument.

3. RESULTS AND DISCUSSION

3.1. Effect of CA on *E.coli* Growth

In order to investigate the influence of CA on *E. coli* growth, the minimum concentration of CA needed for inhibition of *E.coli* growth was obtained via addition of different concentrations of CA to media containing the same *E.coli* concentration. As can be seen in Figure S1 (Supporting Information), concentrations of CA above the 500 mg L^{-1} threshold result in total inhibition of *E.coli* at an initial concentration of 10^5 CFU mL^{-1} in LB media.

The influence of sub-lethal doses of CA (100 mg L^{-1}) on bacteria growth was also studied and compared with control samples. Bacterial growth was observed through lag phase, exponential phase, and stationary phase. For the system under study, a slow growth of *E.coli* was observed for 3 hours after incubation. The bacteria then proceeded to enter its exponential phase for a subsequent 12 hour period. Lastly, exponential growth was observed to stop in batch cultures, indicating the bacteria reached its stationary stage. Figure S2 (Supporting Information) demonstrates the growth curve of *E.coli* at control conditions in comparison to samples where CA was added in sub-lethal concentrations. At sub-lethal concentrations of CA, the rate of bacterial growth was observed to decrease during the lag phase, which was prolonged for 6 hours in comparison to the control culture; following this period, bacteria cultures were observed to achieve stable growth after adaptation to the new environment.

As described in the Experimental section, CA was also added to bacteria culture at different incubation time points. In the case of bacteria treated with CA at lethal concentrations (above

11

MIC), immediately after cell incubation, no bacteria were observed to appear on the agar gel plating during growth, indicating that at the established concentrations, CA completely inhibited bacterial growth. CA, as an antibacterial agent containing an aldehyde group in its structure conjugated to a carbon double bond with a highly electronegative arrangement, interferes with biological processes involving electron transfers. It covalently binds with nitrogen-containing structures such as DNA and proteins via their amine groups, thus extinguishing the metabolic functions of *E.coli*.[18] The polarity of this bond makes the carbon atom electrophilic and reactive to nucleophiles such as primary amines; it also reacts with oxygen-, sulfur-, or nitrogen-centered nucleophiles, resulting in carbamates, thiocarbamates, or thiourea derivatives, respectively, under mild conditions.

3.2. *E.coli* Metabolic Profiling

To monitor the metabolic stress response of *E.coli* exposed to CA, samples treated with different conditions were taken from different stages of the growth curve for analysis, followed by subsequent analysis of changes in metabolic profiling between treated and control *E.coli* samples. According to the obtained results, the highest numbers of features were obtained during the exponential phase of the control samples: 83722 and 77382 features in positive and negative modes, respectively. The features of all chromatographic peaks were extracted for the discovery of discriminative metabolites during bacteria growth.

The trends in the obtained metabolite profiles are observed to change at different growth phases, as shown in Figure S3 (Supporting Information). For instance, levels of amino acids such as phenylalanine or serine were observed to increase during the lag phase, and then decrease during the log phase, while for other amino acids, such as threonine, isoleucine, and valine, values were observed to increase by time. Increased levels of most amino acids during the stationary phase may suggest an enhancement in enzymatic activity related to protein degradation. Changes in the lipid composition of bacteria were also observed during *E.coli* growth, especially for fatty acids and phospholipids; throughout the *E.coli* growth cycle, levels of saturated fatty acids (SFAs) such

as myristic acid and palmitic acid were observed to increase, while levels of unsaturated fatty acids (UFAs) such as palmitoleic acid were observed to decrease. Moreover, increases in cyclopropane fatty acids such as cis-9,10 methylene hexadecanoic acid, and 11-R 12-S methylene octadecanoic acid were observed to occur during the *E.coli* growth cycle, further validating previous finding about accumulation of cyclopropane fatty acids as a result of microorganism growth for microorganisms such as *Serratia marcescens, Lactobacillus* sp., and *E.coli* has been previously reported by Kates et al.[26] In addition, levels of phospholipids such as phosphatydil glycerol (PGs) were also observed to decrease, while phosphatidylethanolamine acid (PEs) levels correspondingly decreased. Previous work has indicated that the observed decrease in UFAs during the growth cycle of *E.coli* could be attributed to their conversion to cyclopropane fatty acids, while the observed decrease in PGs levels may be connected to their conversion to cardiolipin.[27] Cardiolipin is involved in the transfer of phosphatidyl functional groups from one PG to the hydroxyl group of another PG.[27] It is likely that the observed metabolic alterations are linked to bacteria adaptation to new media conditions due to the increase in bacteria numbers during growth.

3.3. Identification of Discriminating Compounds Related to *E. coli* Growth Under CA Treatment Below MIC

To characterize the metabolic response of *E.coli* to CA as an antibacterial agent, comparisons of signal abundance in control versus treated groups were conducted for CA at two different concentrations, below and above the minimum inhibitory concentration (MIC=500 mg L^{-1}), 100 mg L^{-1} and 2000 mg L^{-1}, respectively. For this purpose, different types of experiments were designed so as to evaluate results in terms of different errors (biological or nonbiological), as well as explain significant biological differences with higher confidence. Biological replicates were prepared for *E.coli* samples grown and treated under the same conditions in different 96-well

plates so as to monitor possible biological variability. Moreover, technical replicates were performed in order to determine experimental error attributed to the analytical techniques employed (SPME, MS, and LC methods). The obtained results indicated a variation of less than 10% RSD for the technical analytical approach, and less than 20% for biological replicates.

Trends in metabolite profiles by time were observed for both concentrations of CA. Metabolic variations for both immediate CA addition, and CA addition to growing cultures at different time intervals were also investigated.

Figure S4 (Supporting Information) presents metabolic profiles of bacteria affected by CA at 100 mg L^{-1}, and Figure 1 indicates the heat map of statistically significant metabolites at P < 0.001 based on comparison the control samples in comparison to the cinnamaldehyde treatment samples at below MIC condition (added to growing media immediately after incubation at each individual time point). Results showed an increase in levels of amino acids for samples treated with CA at MIC, while levels of metabolites related to the TCA cycle such as fumaric acid, malic acid, and glucose 6-phosphate were observed to decrease, indicating down-regulation of TCA cycle metabolism. Levels of SFAs were observed to increase while USFAs levels were observed to decrease demonstrating transformation in SFAs to unstaturated ones, resulting in prolonged bacteria life time likely attributed to increasing cell membrane fluidity in stress conditions. An increase in levels of cyclopropane fatty acids such as cis-9,10 methylene hexadecanoic acid, and 11-R 12-S methylene octadecanoic acid was observed to occur in relation to CA addition. Karkas et al. reported that at severe environmental conditions, small amounts of cyclopropane fatty acids were produced to protect the double bond of fatty acids from oxidation.[28] Other studies have also shown an increase in these metabolites as a function of bacteria growth at high temperature conditions.[29,30] In the present work, the observed increase in cyclopropane fatty acids by CA addition could support the evidence of bacteria adaptation to newly introduced harsh conditions.

In addition, increases in levels of N-methylated amino acids such as proline were observed to occur. *E.coli* responds to CA addition as a stress factor by adjusting its membrane composition

through the production of n-methylated amino acids such as proline, which function to maintain cell turgor by osmotic regulation and redox metabolism to eliminate excess amounts of reactive oxygen species (Figure S4 (Supporting Information)). N-methylated amino acids produced by a new class of genes called *osm* (osmotic tolerance) were introduced as potent osmoprotectants and anti-stress activity regulators against dehydration in bacteria by Le Rudulier et al. [31] The potential of these metabolites in the presence of naturally occurring compounds in bacteria environment was confirmed through the introduction of CA in growing bacteria. The cell membrane is the first target of CA, as this compound can change membrane permeability as well as protein functions embedded inside the membrane. Lambert et al. and Burt et al. reported that in the presence of sub-lethal concentrations of naturally occurring antibacterial agents, bacteria reacts by overexpressing stress-response proteins to repair damaged proteins; however, at lethal concentrations, this response is unable to prevent cell death.[13,14]

3.4. Potential Biomarkers in the Case of *E.coli* Treatment by CA above MIC

No bacteria growth was observed for bacteria cultures treated with CA above MIC immediately after incubation (t=0). Growing bacteria cultures treated with CA above MIC every 3 hours after inoculation were sampled every 60 minutes following CA addition. PCA score plots (Figure 2 and Figure 3) are used to demonstrate variability in biological replicates. These plots shows clear separation between extractions performed for treated *E.coli* groups and controls, as well as extractions conducted between different incubation times, in addition to good clustering of QC samples tightly located in the middle, demonstrating good reproducibility of analysis for this metabolomics study for both positive and negative electrospray ionization modes. Two principal components explain 64% of the variance; PC1 51% and PC2 13% for positive ESI, and PC1 45% and PC2 12% for a total negative ESI of 57%. PCA was applied in order to control the quality of the data while PLS-DA was performed to discriminate between control and treatment samples. Figure S5 (Supporting Information) demonstrates clear separation among control and treatment

samples (above MIC), 6 and 12 hours after incubation, which are exponential phase and stationary phase, respectively.

Metabolic profiling of *E.coli* before perturbation at different time points demonstrated significant metabolic changes. Furthermore, the metabolic profiles of bacteria treated by CA under MIC showed significant differentiation from samples treated with sequential addition of CA levels above MIC threshold. Individual clusters were found to contain samples corresponding to different time points and different CA dosing regimens, demonstrating that different pathways of bacterial metabolome are affected by application of CA at different stages of *E. coli* growth.

Hierarchical clustering analysis dendrogram showing the relationship between control samples and cinnmaldehyde treatment samples (above MIC) for different biological replicates at stationary phase is demonstrated at Figure S6 (Supporting Information).

A total of 41 up- and 32 down-regulated metabolites were detected (p-value < 0.0001) for samples dosed with CA above MIC treatment levels. The list of identified compounds is provided in Table 1. Data analysis demonstrated that CA addition above MIC inhibited the metabolism of *E.coli* via different mechanisms, such as inhibition of enzyme-catalyzed reactions, inhibition of cell membrane synthesis following cell lysis and cell death, inhibition of protein synthesis, and protein disruption, which cause disruption of essential enzymatic synthesis, as well as interaction with plasma membranes, consequently affecting membrane permeability as well as metabolism inhibition. Comparisons of profiles yielded significant differentiation in the metabolic pathways of bacteria treated with CA. Based on the obtained results, it can be concluded that introduction of lethal doses of CA disrupts different metabolic pathways such as fatty acids, phospholipids, amino acids, peptides, glycolysis, as well as the TCA cycle, which is discussed in the following section. To the best of this author's knowledge, this is the first time that some of the observed changes in the metabolic pathway of *E.coli* as a function of CA dosing are reported in the literature.

3.4.1. Changes in Membrane Lipids

Results related to comparisons of extractions conducted at different time points of the *E.coli* growth curve using two concentration levels of CA indicated significant differences between the growth curve course and the obtained metabolite profiles. Of note, the metabolic profile of lipids has been observed to significantly differ under different stress conditions in relation to time points and concentration levels. The cytoplasmic membrane of *E.coli* consists of phospholipids containing three fatty acids: palmitic (hexadecanoic) acid as a SFA, as well palmitoleic (hexadecenoic) acid and cis-vaccenic (cis-11-octadecenoic) acid as USFAs.[32] The concurrent changes in USFA concentration levels, in conjunction with the observed decrease in SFA levels in under-MIC CA-treated cultures, can be attributed as principal factors related to changes in the obtained lipid profile; levels of palmitic acid and docosanoic acid, SFAs, were observed to decrease, while an increase in the level of palmitoleic acid, an USFA, was observed to occur. This may suggest up-regulation of desaturase enzyme to increase membrane fluidity through changing SFAs to USFAs. A metabolic pathway investigation indicated that at sub-lethal concentrations of CA, the desaturase enzyme caused an increase in membrane fluidity by promoting changes in SFAs to USFAs. In the presence of stress conditions, cells maintain membrane fluidity by recruiting USFAs as membrane phospholipids. Desaturase enzyme produces USFAs by transferring two hydrogen atoms to oxygen, allowing microorganisms to remain alive longer through the maintenance of membrane structure and function.[33] The consequent increase in bacteria resistance due to this adaptation can be clearly observed through a comparison between the growth curves of *E.coli* treated with sub-lethal CA concentrations and *E.coli* control groups. However, *E.coli* response to CA was noted to differ at lethal CA concentrations. In this condition, levels of metabolites such as USFAs 8-methylnonenoate, 7-oxo-11E-tetradecenoic acid, 7-oxo-11E-tetradecenoic acid, fumarylacetic acid, 6,8,10,12-pentadecatetraenal, 9,10-dihydroxy-12-octadecenoic acid, 3,5,7-trimethyl-undecatetraene, hexadecatetraenoic acid, dodecadienoic acid, and hydroxyl fatty acids such as α-hydroxy myristic acid, myristoyl-EA, and 2-hydroxy capric acid were observed to decrease, while SFA concentrations of 2-keto palmitic acid was observed to

increase concurrently. This observation is in accordance with previous findings about the ability of CA to damage cell membranes. Increase of USFAs is known to induce decrease in cell membrane fluidity, respiratory activity, coagulation of cytoplasmic materials, and eventually lead to cell lysis and leakage of macromolecules.[33-38] In addition, the newly determined change in the metabolic pathway of CA-treated *E.coli*, observed by significant up-regulation in lysophosphatidylserine, could be related to phospholipase or carboxylic ester hydrolase inactivation, which could be attributed to the interaction of CA by lipid membrane.

3.4.2. Changes in Amino acids

The observed increase in levels of amino acids and peptides such as lysine, tyrosyl-alanine, glutamyl-hydroxyproline, 2-hydroxymethylserine, n-(6)-[(Indol-3-yl)acetyl] lysine, phenylacetylglycine, lysopine, histidine, 5-methoxytryptophan, phenylalanylproline, 3-(phosphoacetylamido) alanine, threonine, glutamine, and prolylhydroxyproline could be attributed to protein denaturing and inhibition of protein synthesis, which is caused by a halt in the synthesis of essential enzymes as a result of the addition of CA. On the other hand, a comparison of changes in metabolite levels between CA-treated bacteria and control bacteria demonstrated that this compound can perturb enzyme-catalyzed reactions such as glutathione, arginine decarboxylase, and histidine decarboxylase. For example, increases in riboflavin and histidine could be attributed to the interruption of histidine decarboxylase action. Conversely, a decrease in the agmatine metabolite may be caused by the inhibition of arginine decarboxylase by CA. Agmatine is the resulting product from the decarboxylation of arginine through the action arginine decarboxylase enzyme.[39] These results support previous findings that demonstrated the inhibitory activity of CA for some enzymes including histidine decarboxylase and arginine decarboxylase, leading to accumulation of amino acids.[39,40]

3.4.3. Inhibition of Glycolysis Pathway

18

The obtained results indicated that CA could also dysregulate the citrate metabolic pathway, consequently influencing enzymes involved in ATP synthesis. Accumulation of glucose indicates down-regulation of the catabolic pathway in bacteria affected by CA, and lead to failure in ATP formation – the main source of energy. Previous studies confirmed that diffusion of CA to the cell periplasm induce a decrease in ATPase activity of cell membrane.[41,42] Consequently, without energy production, cells loss their viability.[43]

Therefore, CA was recognized as an interesting candidate for cancer treatment due to its natural occurrence and its ability to inhibit glycolysis, since most cancer cells use ATP-derived from glucose catabolism as energy source.[44]

3.4.4. Changes in Other Metabolites

Based on the obtained result, increases in cyclic CMP, which can be related to inhibition of CMP kinase activity due to interruption of the phosphorylation mechanism in CA treated bacteria revealed in the presented work. Accumulation of carnitine accompanied by down-regulation of glycine betaine could be directly linked to inhibition of various catabolic enzymes such as carnitine dehydrogenase. The carnitine pathway may play more than one role in cell function; in addition to generation of an osmoprotectant (glycine betaine), carnitine may play a role in the generation of an external electron acceptor in anaerobic respiration. Moreover, glycine betaine levels were observed to decrease in *E.coli* under administration of above-MIC CA levels, suggesting that CA may impair the glycine betaine pathway in which choline dehydrogenase is involved. Strøm et al. introduced glycine betaine as an osmoprotectant in *E.coli* under stress conditions induced by addition of salt and exposure to cold.[45] In our present study, the observed results indicated that under administration of CA above MIC levels, this metabolite was unable to preserve cell turgor.

Other down-regulated metabolites such as myo-inositol 3-triphosphate and phytic acid were also indicated as discriminant compounds for the present study. Phytase (myo-inositol hexakisphosphate phosphohydrolase) is classified as a phosphatase enzyme that catalyzes phytic

acid hydrolysis as a source of phosphorous.[46,47] This type of change in metabolome profile infers inhibition of phytase activity in CA-treated sample. Our study indicated that CA could stop enzymatic activity while concurrently blocking the nitrogen or carbonyl terminal of proteins through covalent bonds. Upregulation of carnitine also could be representative of enhancement in fatty acids β-oxidation as an alternative energy supply.

Another enzyme inferred to be affected due to CA addition in growing bacteria media is glutathione S-transferase, known to catalyze the addition of glutathione thiol groups to suitable electrophilic species. This enzyme is responsible for producing reduced glutathione by catalyzing the conjugation of electrophilic compounds. Glutathione S-transferase is responsible for detoxification of reactive oxygen species through decreasing peroxide levels to increase bacterial survival. Kanai et al. reported three distinct types of glutathione S-transferase from *E.coli* with defensive characteristics against oxidative stress (hydrogen peroxide).[48] The presented research work demonstrated that CA influences glutathione S-transferase activity; the same observation has been previously reported in the literature for *E.coli* treated by hydrogen peroxide, showing that CA acts as an oxidative agent.

3.4.5. Anti-Quorum Sensing Activity

Quorum sensing, defined as gene expression regulation in response to cell population fluctuation, is the phenomena in which bacteria secrets auto-inducers; when these compounds reach their threshold level, their interaction with transcriptional regulators affects gene expression.[49] Enzymatic degradation of signaling molecules inhibits biofilm formation in systematic and local infections, pathogenicity, and antibiotic resistance. In this study, we observed the significant down-regulation of signal molecules such as N-decanoyl-L-homoserine lactone and N-tetradecanoyl-L-homoserine lactone levels produced by microorganism in CA treated media. Decrease in the levels of these two signaling molecules may be related to the disruption of cell-to-cell communication, and then lead to inhibition of biofilm formation. Quorum sensing is known to contribute significantly to the resistance and virulence of *E.coli*. The anti-quorum sensing activity of CA was already proposed by

Urbanowski et al.[50] The authors suggested that CA or one of its metabolites act as antagonist to autoinducer receptor binding.

The above-mentioned changes in the metabolic pathways due to response of *E.coli* to CA treatment provide evidences of multi-functional role of this natural compound as antibacterial agent. The obtained results demonstrated that SPME is a sensitive tool for in vivo metabolomics analysis enabling obtaining time-resolved data without the need of sample collection thus no disturbance of living systems. This approach may be successfully applied for monitoring of metabolic pathways towards discovery of molecules which can serve as significantly differentiate metabolites or improving the knowledge on mechanisms that pathogens react to newly discovered compounds in drug discovery and development.

4. CONCLUSION

In this research, SPME-LC-MS platform was used for the first time due for investigation of bacterial metabolome to provide time-resolved information about changes induced by different doses of natural antibacterial agent, cinnamaldehyde (CA), at different stages of the pathogen growth. Numerous discriminant metabolites were identified using the technique and provided further insight into metabolic pathways alteration in *E.coli* culture. Among compounds influenced by CA were those related to TCA cycle, fatty acids, glycolysis, amino acids metabolism, cell membrane, and protein synthesis. Based on the up-regulation and down-regulation in the above-mentioned metabolite levels of treatment samples versus control samples, CA influences many enzymes involved in protein interactomes. The developed SPME-LC-MS method assists in the evaluation of metabolome changes, and the results of the current work could contribute to the field by obtaining more knowledge regarding endogenous and exogenous molecules participating in molecular binding including proteins, nucleic acids, carbohydrates, lipids and drugs. Based on the results obtained from metabolic profiling investigation, low level concentration of CA interacts with membrane and proteins embedded inside while higher levels of CA can diffuse

inside the cell and affect the cytoplasmic enzymes and transcriptome. Moreover, the latter condition disrupts the membrane and cause cell death. The proposed approach may offer additional opportunities to food microbiologists for evaluation of metabolic pathways involved in growth and survival of pathogens in foods, food processing environments as well as humans.

ASSOCIATED CONTENT

Supporting Information

Figure S1. Investigation of MIC of cinnamaldehyde on *E.coli* (10^5 CFU ml^{-1}) growth.
Figure S2. *E.coli* growth curves for control sample, and CA treated bacteria at sublethal concentration.
Figure S3. Statistically significant changed metabolites (p<0.001) during *E.coli* growth (control samples).
Figure S4. Statistically significant metabolite changes (p<0.001) during *E.coli* treated samples growth curve (under MIC).
Figure S5. PLS score plot discrimination between experimental groups (control (c) and treated samples above MIC (cc) at two different time points.
Figure S6. Hierarchical clustering analysis heatmap of bacteria dataset.

REFERENCES
(1) Koek, M.M.; Muilwijk, B.; Van der Werf, M. J.; Hankemeier, T. Microbial metabolomics with gas chromatography/mass spectrometry. Anal Chem. **2006**, 78, 1272-1281.
(2) Tautenhahn, R.; Patti, G. J.; Kalisiak, E.; Miyamoto, T.; Schmidt, M.; Lo, F. Y.; McBee, J.; Baliga, N. S.; Siuzdak, G. metaXCMS: second-order analysis of untargeted metabolomics data. Anal. Chem. **2011**, 83, 696–700.
(3) Zhang, A. H.; Sun, H.; Han, Y.; Yan, G.; Yuan, Y.; Song, G. C.; Yuan, X.; Xie, N.; Wang, X. Stable Isotope-Assisted Metabolomics for Network-Wide Metabolic Pathway Elucidation. Anal. Chem. **2012**, 84, 8442−8447.
(4) Dunn, W. B.; Broadhurst, D.; Begley, P.; Zelena, E.; Francis-McIntyre, S.; Anderson, N.; Brown, M.; Knowles, J. D.; Halsall, A.; Haselden, J. N.; Nicholls, A. W.; Wilson, I. D.; Kell, D.

B.; Goodacre, R. Procedures for large-scale metabolic profiling of serum and plasma using gas chromatography and liquid chromatography coupled to mass spectrometry. Nature protocols 2011, 6, 1060 -1083.

(5) Wu, Y.; Li, L. Development of Isotope Labeling Liquid Chromatography–Mass Spectrometry for Metabolic Profiling of Bacterial Cells and Its Application for Bacterial Differentiation. Anal Chem. 2013, 85, 5755-5763.

(6) Annous, B. A.; Fratamico, P. M.; Smith, J. L. Quorum Sensing in Biofilms: Why Bacteria Behave the Way They Do. J. Food science. 2009, 74, R24-R37.

(7) Marcus, C.; Lichtenstein, E.P. Biologically active components of anise: toxicity and interactions with insecticides in insects. J. Agric. Food Chem. **1979**, 27, 1217–1223.

(8) Bruni, R.; Medici, A.; Andreotti, E.; Fantin, C.; Muzzoli, M.; Dehesa, M. Chemical composition and biological activities of Ishpingo essential oil, a traditional Ecuadorian spice from *Ocotea quixos* (Lam.) Kosterm. (Lauraceae) flower calices. Food Chem. 2003, 85, 415–421.

(9) Sacchetti, G.; Maietti, S.; Muzzoli, M.; Scaglianti, M.; Manfredini, S.; Radice, M.; Bruni, R. Comparative evaluation of 11 essential oils of different origin as functional antioxidants, antiradicals and antimicrobials in foods. Food Chem. **2005**, 91, 621–632.

(10) Bakkali, F.; Averbeck, S.; Averbeck, D.; Idaomar, M. Biological effects of essential oils – A review. Food and Chemical Toxicology. 2008, 46, 446–475.

(11) Hyldgaard, M.; Mygind, T.; Meyer, R.L. Essential oils in food preservation: mode of action, synergies, and interactions with food matrix components. Frontiers in Microbiology, **2012**, 3, 1-24.

(12) Jozefczuk, S.; Klie, S.; Catchpole, G.; Szyanski, J.; Cuadros-Inostroza, A.; Steinhauser, D.; Selbig, J.; Willmitzer, L. Metabolomic and transcriptomic stress response of Escherichia coli. Molecular system biology **2010**, 6, 1-16.

(13) Lambert, R.J.W.; Skandamis, P.N.; Coote, P.J.; Nychas, G.J.E. A study of the minimum inhibitory concentration and mode of action of oregano essential oil, thymol and carvacrol. J. Appl. Microbiol. 2001, 91, 453-462.

(14) Burt, S.A.; van der Zee, R.; Koets, A.P.; de Graaff, A.M.; van Knapen, F.; Gaastra, W.; Haagsman, H.P.; Veldhuizen, E.J.A. Carvacrol induces heat shock protein 60 and inhibits synthesis of flagellin in Escherichia coli O157:H7. Appl. Environ. Microbiol. **2007**, 73, 4484–4490.

(15) Suresh, P.; Ingle, V. K.; Vijaya Lakshmi, V. Antimicrobial Activity of Essential Oils from Spices Against Psychrotrophic Food Spoilage Microorganisms. J. Food Sci Technol. **1992**, 29, 254-256.

(16) Bilgrami, K.S.; Sinha, K. K.; Sinha, A. K. Inhibibition of aflatoxin production & growth of Aspergillus flavus by eugenol & onion &garlic extracts. Indian J Med Res, **1992**, 96, 171-175.

(17) Pacheco, P.; Sierra, J.; Schmeda-Hirschmann, G.; Potter, C. W.; Jones, B. M.; Moshref, M. Antiviral activity of chilean medicinal plant extracts. Phytother Res. **1993**, 7, 415-418.

(18) Nazzaro, F.; Fratianni, F.; Martino, L.D.; Coppola, R.; De Feo, V. Effect of Essential Oils on Pathogenic Bacteria. Pharmaceuticals **2013**, 6, 1451-1474.

(19) Yanes, O.; Tautenhahn, R.; Patti, G. J.; Siuzdak, G. Expanding Coverage of the Metabolome for Global Metabolite Profiling. Anal. Chem. 2011, 83, 2152-2161.

(20) Bessonneau, V.; Bojko, B.; Pawliszyn, J. Analysis of human saliva metabolome by direct immersion solid-phase microextraction LC and benchtop orbitrap MS. Bioanalysis. 2013, 5 (7) 783-792.

(21) Bojko, B.; Reyes-Garces, N.; Bessonneau, V.; Gorynski, K.; Mousavi, F.; Silva, E.; Pawliszyn, J. Solid-phase microextraction in metabolomics, TrAC Trends in Analytical Chemistry, 2014, 61, 168-180.

(22) Vuckovic, D. Doctoral thesis, University of Waterloo, **2010**, Chapter 1.

(23) Hossain, S.M. Z.; Bojko, B.; Pawliszyn, J. Automated SPME–GC–MS monitoring of headspace metabolomic responses of E. coli to biologically active components extracted by the coating. Analytica Chimica Acta. **2013**, 776, 41-49.

(24) Mousavi, F.; Bojko, B.; Pawliszyn, J. Optimization of the coating procedure for a high-throughput 96-blade solid phase microextraction system coupled with LC-MS/MS for analysis of complex samples. Analytica Chimica Acta. 2015, 892, 95-104.

(25) Mirnaghi, F. S.; Chen, Y.; Sidisky, L.M.; Pawliszyn, J. Optimization of the coating procedure for a high-throughput 96-blade solid phase microextraction system coupled with LC-MS/MS for analysis of complex samples. J. Anal. Chem. 2011, 83, 6018-6025.

(26) Kates M. Bacterial lipids. Adv. Lipid Res. **1964**, 2, 17-90.

(27) Cronan, J.R.J.E. Phospholipid Alterations During Growth of *Escherichia coli.* J. Bacteriol. 1968, 95, 2054-2061.

(28) Karkas, J.; Türler, H.; Chargaff, E. Studies on the specification of accessory biochemical characters, as exemplified by the fatty acid patterns of various strains of Escherchia coli. Biochim. Biophys. Acta. **1965**, 111, 96-109.

(29) Knivett, V., Cullen. J. Phospholipid Alterations During Growth of *Escherichia coli.* J. Biochem. **1965**, 96, 771-776.

(30) Marr, A. G.; Ingraham, J.L. Effect of temperature on the composition of fatty acids in Escherichia Coli. J. Bacteriol. 1962, 84, 1260-1267.

(31) Le Rudulier, D.; Strϕm, A. R.; Dandekar, A. M.; Smith, L.T.; Valentine, R. Molecular Biology of Osmoregulation. Science 1984, 224, 1064-1068

(32) Di PasquaI, R.; Hoskins, N.; Betts, G.; Mauriello, G. Membrane toxicity of antimicrobial compounds from essential oils. J. Agric. Food Chem. **2006**, 54, 2745-2749.

(33) Russell, N. J. Mechanism of thermal adaptation in bacteria: Blueprints for survival. Trends Biochem. Sci. **1984**, 9,108-112.

(34) Bayer, A. S.; Presad, R.; Chandra, J.; Smirti, A.M.; Varma, A.,; Skurray, R.A.; Firth, N.; Brown, M.H.; Koo, S.P.; Yeaman, M.R. In Vitro Resistance of *Staphylococcus aureus* to Thrombin-Induced Platelet Microbicidal Protein Is Associated with Alterations in Cytoplasmic Membrane Fluidity. Infect. Immun. **2000**, 68, 3548–3553.

(35) Russell, N.J., Psychrophilic bacteria-molecular adaptations of membrane lipids. Comp. Biochem. Physiol. **1997**, 118, 489-493.

(36) Di Pasqua, R.; Betts, G.; Hoskins, N.; Edwards, M.; Ercolini, D.; Mauriello, G. Membrane toxicity of antimicrobial compounds from essential oils. J. Agric. Food Chem. **2007**, 55, 4863–4870.

(37) Gustafson, J.E.; Liew, Y.C.; Chew, S.; Markham, J.L.; Bell, H.C.; Wyllie, S.G.; Warmington, J.R. Effects of tea tree oil on Escherichia coli. Lett. Appl. Microbiol. **1998**, 26, 194-198.

(38) Oussalah, M.; Gaillet, S.; Lacroix, M. Mechanism of Action of Spanish Oregano, Chinese Cinnamon, and Savory Essential Oils against Cell Membranes and Walls of *Escherichia coli O157:H7* and Listeria monocytogenes. J. Food Prot. **2006**, 69, 1046-1055.

(39) Auger, E.A.; Redding, K. E.; Plumb, T.; Childs, L. C.; Meng, S. Y.; Bennett, G. N. Construction of lac fusions to the inducible arginine- and lysine decarboxylase genes of Escherichia coli K12. Mol. Microbiol. **1989**, 3, 609– 620.

(40) Wendakoon, C. N.; Sakaguchi, M. Inhibition of amino acid decarboxylase activity of Enterobacter aerogenes by active components in spices. J. Food Protection **1995**, 58, 280-283.

(41) Gill, A.O.; Holley, R.A. Disruption of Escherichia coli, Listeria monocytogenes and Lactobacillus sakei cellular membranes by plant oil aromatics. Int. J. Food Microbiol. **2006a**, 108, 1-9.

(42) Gill, A.O.; Holley, R.A. Inhibition of membrane bound ATPases of Escherichia coli and Listeria monocytogenes by plant oil aromatics. Int. J. Food Microbiol. **2006b**, 111, 170-174.

(43) Picone, G.; Laghi, L.; Gardini, F.; Lanciotti, R.; Siroli, L.; Capozzi, F. Evaluation of the effect of carvacrol on the Escherichia coli 555 metabolome by using 1H-NMR spectroscopy. Food Chem. **2013**, 141, 4367–4374.

(44) Pelicano, H.; Martin, D.S.; Xu, R.H.; Huang, P. Glycolysis inhibition for anticancer treatment. Oncogene. **2006**, 25, 4633–4646.

(45) Strφm, A. R. Osmoregulation in the model organism Escherichia coli: genes governing synthesis of glycine betaine and trehalose and their use in metabolic engineering of stress tolerance. J. Biosci. **1998**, 23, 437-445.

(46) Mullaney, E. J.; Daly, C.B.; Ullah, A.H. Advances in phytase research. Adv Appl Microbiol. **2000**, 47, 157–199.

(47) Mullaney, E.J., Ullah, A.H. The term phytase comprises several different classes of enzymes. Biochem Biophys Res Commun. 2003, 312, 179–184.

(48) Kanai, T.; Takahashi, K.; Inoue, H. Three distinct-type glutathione *S*-transferases from *Escherichia coli* important for defense against oxidative stress. J. Biochem. 2006, 140, 703–711.

(49) Niu, C.; Afre, S.; Gilbert, E.S. Subinhibitory concentrations of cinnamaldehyde interfere with quorum sensing. Letters in Applied Microbiology 2006, 43, 489–494.

(50) Urbanowski, M. L.; Lostroh, C.P.; Greenderg, E.P. Reversible Acyl-Homoserine Lactone Binding to Purified *Vibrio fischeri* LuxR Protein. J. Bacteriol. 2004, 186, 631-637.

Table 1. Statistically significant differentiated metabolites between CA treated bacteria above MIC added every 3 hours after incubation and control *E.coli* sample (metabolites confirmed by retention time and fragmentation pattern matching with commercially available reference standards are highlighted in **bold**). Mass accuracy of the measurement is defined as the ratio of mass error (difference between experimentally measured mass (mz (expr.)) and exact theoretical mass (mz (theor.)) and can be calculated using the following equation:

mass accuracy (ppm)= (Regulation:⬜⬜;Up-regulated:⬜;Down-regulated: ⬜)

Metabolite	Chemical formula	METLIN ID	Class	P value	mz (theor.)	RT (min)	mz (expr.)	⬜⬜	Adduct	Mass accuracy (ppm)	Main fragments
Betaine aldehyde	$C_5H_{11}NO$	278	Alkylamines	0.00062	102.0918	0.86	102.0910	⬜	M+ H	-7.8	58.0662; 59.0734
n(6)-[(indol-3-yl)acetyl]-L-lysine	$C_{16}H_{21}N_3O_3$	66141	Amino Acids and Derivatives	5.95920e-7	304.1661	3.35	304.1660	⬜	M+H	-0.3	-----------
Glycine betaine	$C_5H_{11}NO_2$	287	Amino Acids and Derivatives	7.81195e-7	118.0868	0.86	118.0866	⬜	M+H	-1.7	58.0662; 59.0736
Methionine	$C_5H_{11}NO_2S$	26	Amino acids and derivatives	1.16363e-6	150.0588	0.98	150.0584	⬜	M+H	-2.6	56.0502; 61.0114; 104.0525; 133.0312
Phytic acid	$C_6H_{18}O_{24}P_6$	4238	Cyclic alcohols and derivatives	0.00047	698.8250	2.56	698.8250	⬜	M+K	0	80.9719; 98.9835; 462.891; 642.8589
myo-inositol 3-triphosphate	$C_6H_{13}O_9P$	359	Cyclic alcohols and derivatives	3.83342e-6	261.0375	1.01	261.0372	⬜	M+ H	-1.1	241.0102, 138.9731
8-methylnonenoate	$C_{10}H_{17}O_2$	62842	Fatty Acids and Conjugates	1.55983e-10	170.1306	6.84	170.1304	⬜	M+H	-6.9	-----------
7-oxo-11E-tetradecenoic acid	$C_{14}H_{24}O_3$	45868	Fatty Acids and Conjugates	1.65801e-6	241.1803	6.07	241.1804	⬜	M+H	0.6	-----------
Fumarylacetic acid	$C_6H_6O_5$	45910	Fatty Acids and Conjugates	1.27344e-6	181.0112	0.98	181.0101	⬜	M+Na	-6.1	-----------
6,8,10,12-pentadecatetraenal	$C_{15}H_{22}O$	91269	Fatty Acids and Conjugates	6.71761e-6	241.1568	4.84	241.1563	⬜	M+ Na	-2.1	-----------
9,10-dihydroxy-12-	$C_{18}H_{34}O_4$	35501	Fatty Acids and	9.52547e-7	337.2354	8.16	337.2351	⬜	M+Na	-0.9	229.1573;

octadecenoic acid			Conjugates								163.1359
3,5,7-trimethyl-undecatetraene	$C_{14}H_{22}$	97470	Fatty Acids and Conjugates	0.00024	191.1799	6.12	191.1793	☐	M+H	-3.1	177.0523; 129.1326
Hexadecatetraenoic acid	$C_{16}H_{24}O_2$	34835	Fatty Acids and Conjugates	0.00055	249.1854	7.08	249.1845	☐	M+H	-3.6	219.1952; 124.0869
13-hexadecenoic acid	$C_{16}H_{30}O_2$	34927	Fatty Acids and Conjugates	6.3251e-6	277.2143	7.11	277.2145	☐	M+Na	0.7	259.1901; 228.2319; 195.1014
Dodecadienoic acid	$C_{12}H_{20}O_2$	34896	Fatty Acids and Conjugates	0.00160	197.1541	5.05	197.1539	☐	M+H	-1.0	137.1325; 109.1011
α-hydroxy myristic acid	$C_{14}H_{28}O_3$	35391	Fatty Acids and Conjugates	3.27691e-7	243.1960	5.16	243.1961	☐	M-H	0.4	197.1911; 169.1590
Myristoyl-EA	$C_{16}H_{33}NO_2$	46563	Fatty Acids and Conjugates	0.00001	310.2148	5.74	310.2136	☐	M+K	-3.8	244.1287; 227.1750; 213.1594
2-hydroxy capric acid	$C_{10}H_{20}O_3$	35411	Fatty Acids and Conjugates	0.00071	187.1334	5.05	187.1338	☐	M-H	2.1	-----------
6-Tridecene	$C_{13}H_{26}$	97873	Fatty Acids and Conjugates	7.33244e-7	181.1956	3.93	181.1955	☐	M-H	-0.6	-----------
2,6-dimethylheptanoyl carnitine	$C_{16}H_{31}NO_4$	58391	Fatty Acid Esters	5.44908e-6	324.2150	4.62	324.2151	☐	M+ Na	0.4	205.0856; 301.1403; 279.1585; 190.0496
9,12-hexadecadienoic acid	$C_{16}H_{28}O_2$	34787	Fatty acyls	0.00086	251.2011	10.53	251.2012	☐	M-H	0.4	-----------
pentadecatetraenal	$C_{15}H_{22}O$	91269	Fatty aldehydes	6.71761e-6	217.1592	4.84	217.1591	☐	M-H	-0.5	-----------
1-nonaDecanol	$C_{19}H_{40}O$	26349	Fatty alcohols	5.83294e-7	283.3000	8.40	283.2999	☐	M-H	-0.4	-----------
Agmatine	$C_5H_{14}N_4$	3523	Guanidines	3.88392e-6	131.1296	1.33	131.1286	☐	M+H	-7.6	60.0549; 72.0812; 114.1025
4-hydroxyindole	C_8H_7NO	34514	Indols	2.36999e-8	134.0605	3.51	134.0605	☐	M+ H	0	115.0542
Methylindole	C_9H_9N	5453	Indols	0.00009	132.0813	5.07	132.0806	☐	M+H	-5.3	77.0394; 89.0401; 103.0545; 117.0574
Guanine	$C_5H_5N_5O$	315	Imizopyrimidines	2.11405e-9	152.0572	0.93	152.0572	☐	M+H	0	135.0302; 110.0358
Creatinine	$C_4H_7N_3O$	8	Lactams	0.00234	114.0667	1.27	114.0662	☐	M+H	-4.4	114.0687, 86.0741
N-decanoyl-L-homoserine lactone	$C_{14}H_{25}NO_3$	45310	---------------	9.41730e-7	256.1912	5.21	256.1923	☐	M+H	4.3	57.0702; 74.0216; 84.0381; 95.0782; 102.0521
N-tetradecanoyl-L-homoserine lactone	$C_{18}H_{33}NO_3$	64716	---------------	9.46201e-7	310.2382	8.40	310.2375	☐	M-H	-2.3	74.0413; 102.0561; 211. 2075
2-hydroxymethylserine	$C_4H_9NO_4$	65894	Amino Acids and Derivatives	2.15173e-7	136.0609	0.93	136.0610	☐	M+ H	0.7	-----------
N2-(D-1-Carboxyethyl)-L-lysine	$C_9H_{18}N_2O_4$	63467	Amino Acids and Derivatives	9.61847e-6	219.1344	1.27	219.1331	☐	M+H	-5.9	-----------
Phenylacetylglycine	$C_{10}H_{11}NO_3$	4237	Amino Acids and Derivatives	6.60221e-7	194.0817	2.82	194.0815	☐	M+H	-1.0	65.0414; 91.0553
5-methoxytryptophan	$C_{12}H_{14}N_2O_3$	103475	Amino Acids and Derivatives	2.47692e-6	257.0902	0.97	257.0901	☐	M+Na	-0.4	-----------
Phenylalanylproline	$C_{14}H_{18}N_2O_3$	23997	Amino Acids and Derivatives	0.00002	263.1395	2.24	263.1393	☐	M+H	-0.8	-----------
3-(phosphoacetylamido)alanine	$C_5H_{11}N_2O_7P$	66116	Amino Acids and Derivatives	0.00001	280.9940	0.89	280.9932	☐	M+K	-2.8	-----------
Proline	$C_5H_9NO_2$	29	Amino acids and derivatives	0.00003	116.0711	0.98	116.0710	☐	M+H	-0.9	70.0662
Aspartic acid	$C_4H_7NO_4$	15	Amino acids and derivatives	0.00001	134.0453	0.88	134.0448	☐	M+H	-0.9	74.0243, 88.0378; 116.0352
Glutamic acid	$C_5H_9NO_4$	19	Amino acids and derivatives	1.4215e-6	148.0609	0.80	148.0604	☐	M+H	-3.4	84.0451; 102.0554; 130.0503
Phenylalanine	$C_9H_{11}NO_2$	28	Amino acids and derivatives	2.2586e-7	166.0868	1.17	166.0868	☐	M+H	0	103.0559; 120.0824
Histidine	$C_6H_9N_3O_2$	21	Amino acids and derivatives	0.00005	156.0773	0.93	156.0769	☐	M+H	-2.5	83.0611; 93.0453; 110.0712

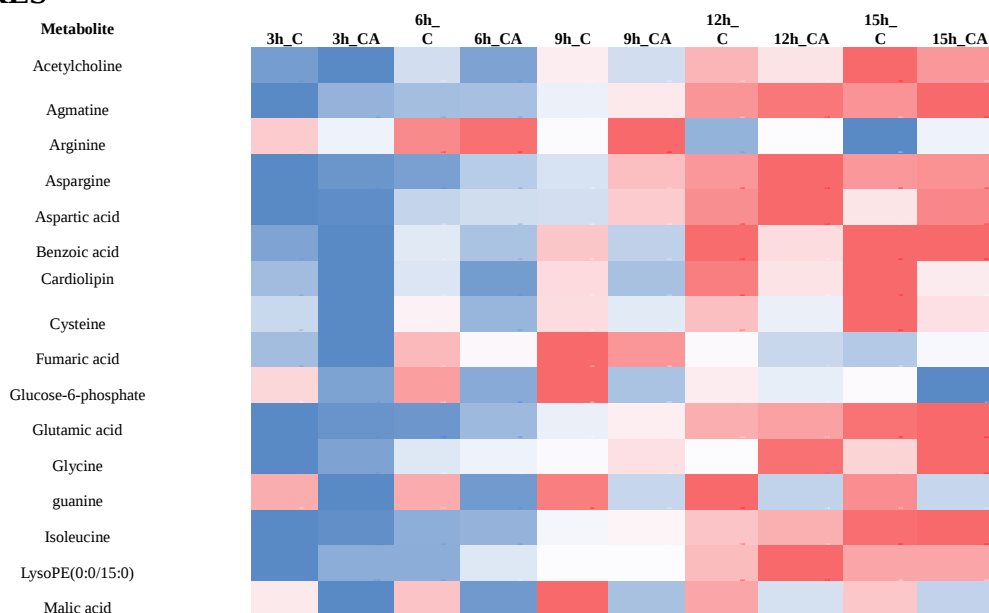| Name	Formula	ID	Category	Value	m/z	RT	m/z theor		Adduct	ppm	Fragments
Arginine	C$_6$H$_{14}$N$_4$O$_2$	13	Amino acids and derivatives	5.0953e-7	175.1195	1.03	175.1189	☐	M+H	-3.4	74.0246; 88.0394; 116.0351
Tryptophan	C$_{11}$H$_{12}$N$_2$O$_2$	33	Amino acids and derivatives	0.000014	205.0977	2.86	205.0972	☐	M+H	-2.4	118.0657; 146.0593; 188.0702
2-hydroxymethylserine	C$_4$H$_9$NO$_4$	65894	Amino Acids and Derivatives	2.15173e-7	136.0609	0.93	136.0610	☐	M+ H	0.7	132.1015
N2-(D-1-carboxyethyl)-L-lysine	C$_9$H$_{18}$N$_2$O$_4$	63467	Amino Acids and Derivatives	9.61847e-6	219.1344	1.27	219.1331	☐	M+H	-5.9	--------------
Phenylacetylglycine	C$_{10}$H$_{11}$NO$_3$	4237	Amino Acids and Derivatives	6.60221e-7	194.0817	2.28	194.0815	☐	M+H	-1.0	153.0544; 125.0597
Valine	C$_5$H$_{11}$NO$_2$	35	Amino acids and derivatives	0.000036	118.0868	2.20	118.0864	☐	M+H	-3.3	118.0868, 72.0815
Isoleucine	C$_6$H$_{13}$NO$_2$	23	Amino acids and derivatives	6.53741e-8	132.1024	1.27	132.1020	☐	M+H	-3.0	132.1018, 86.0968
Cysteine	C$_3$H$_7$NO$_2$S	3757	Amino acids and derivatives	0.000071	122.0275	0.80	122.0275	☐	M+H	0	76.0815; 87.0354; 104.9781
Threonine	C$_4$H$_9$NO$_3$	32	Amino acids and derivatives	0.000033	120.0660	0.93	120.0656	☐	M+H	-3.3	56.0512; 74.0610; 102.0557
Glutamine	C$_5$H$_{10}$N$_2$O$_3$	18	Amino acids and derivatives	4.66183e-6	147.0769	1.15	147.0771	☐	M+H	1.3	84.0454; 130.0492
Lysine	C$_6$H$_{14}$N$_2$O$_2$	71200	Amino Acids and Derivatives	3.52559e-9	147.1133	1.02	147.1129	☐	M+H	-2.7	56.0508; 84.0817; 130.0861
Galactosyl 4-hydroxyproline	C$_{10}$H$_{16}$O	86214	Carboxylic acid and derivatives	1.457687e-6	153.1279	4.21	153.1281	☐	M+H	1.3	149.1323; 119.0855
Carnitine	C$_7$H$_{15}$NO$_3$	63461	Alkylamines	4.45447e-6	162.1130	1.33	162.1131	☐	M+ H	-0.6	60.0814; 85.0291; 103.0392
4-keto lauric acid	C$_{12}$H$_{22}$O$_3$	35733	Fatty Acids and Conjugates	0.00038	215.1647	4.01	215.1644	☐	M+H	1.4	-----------
2-keto palmitic acid	C$_{16}$H$_{30}$O$_3$	35744	Fatty Acids and Conjugates	0.00005	269.2116	5.55	269.2117	☐	M-H	0.4	195.1014; 181.0646; 161.1323; 127.1117
Hexadecanoic acid	C$_{16}$H$_{32}$O$_2$	187	Fatty acyls	0.00086	255.2324	8.20	255.2324	☐	M-H	0	57.0709; 71.0857; 103.0745
Dodecanamide	C$_{12}$H$_{25}$NO	36671	Fatty amides	0.00029	200.2014	6.85	200.2013	☐	M+ H	-0.5	161.1323; 127.1117
PA(13:0/0:0)	C$_{16}$H$_{33}$O$_7$P	3886	Glycerophospholipids	1.36265e-8	367.1885	5.17	367.1884	☐	M-H	-0.3	-----------
PA(P-16:0/20:5(5Z,8Z,11Z,14Z,17Z))	C$_{39}$H$_{67}$O$_7$P	82262	Glycerophospholipids	6.21982e-7	717.4261	5.77	717.4254	☐	M+K	-1.0	572.3438; 501.7861; 445.2444; 333.1038; 264.1591
PE(18:0/12:0)[U]	C$_{35}$H$_{70}$NO$_8$P	40423	Glycerophospholipids	0.00027	664.4917	7.54	664.4898	☐	M+H	-2.9	-----------
LysoPE(0:0/15:0)	C$_{20}$H$_{42}$NO$_7$P	62289	Glycerophospholipids	0.00018	440.2777	5.92	440.2765	☐	M+H	-2.7	-----------
Lysophosphatidylserine	C$_{24}$H$_{48}$NO$_9$P	34531	Glycerophospholipids	0.00005	525.3066	5.92	525.3062	☐	M+	-0.8	526.3134, 508.3015
2-hydroxydecanedioic acid	C$_{10}$H$_{18}$O$_5$	5413	Hydroxy acids and derivatives	1.6437e-7	257.0791	0.95	257.0792	☐	M+K	-0.4	-----------
Glucose	C$_6$H$_{12}$O$_6$	3755	Monosaccharides	6.07467e-6	203.0531	0.77	203.0531	☐	M+Na	0	56.7694; 118.0872; 143.0715
Glutamyl-hydroxyproline	C$_{10}$H$_{11}$N$_5$O$_5$	69076	Peptides	6.80448e-8	282.0838	0.87	282.0821	☐	M+H	-6.0	-----------
Prolylhydroxyproline	C$_{10}$H$_{16}$N$_2$O$_4$	58518	Peptides	6.76841e-6	229.1188	1.15	229.1190	☐	M+H	0.9	197.1281; 135.1013
Tyrosyl-alanine	C$_{12}$H$_{16}$N$_2$O$_4$	85991	Peptides	1.67676e-9	253.1188	1.86	253.1174	☐	M+H	-5.5	---------
Riboflavin (vitamin B2)	C$_{17}$H$_{20}$N$_4$O$_6$	233	Pteridines and derativievs	0.00008	377.1461	1.51	377.1460	☐	M+H	-0.3	172.0872; 198.0651; 243.0895
Cyclic CMP	C$_9$H$_{12}$N$_3$O$_7$P	3436	Pyrimidine nucleotides	7.08504e-6	306.0491	0.78	306.0481	☐	M+H	-3.2	95.024; 112.050
Hexylglutathione	C$_{16}$H$_{29}$N$_3$O$_6$S	24067	--------------	0.00060	392.1855	4.35	392.1854	☐	M+H	-0.3	84.0456; 86.9913; 116.0162

FIGURE CAPTIONS

Figure 1. Heat map of statistically significant metabolic change (p<0.001) between control *E.coli* sample comparison and cinnamaldehyde (under MIC) treated *E.coli* at different time points: #h_C: control sample after inoculation a liquid bacterial culture at # of hours; #h_CA: cinnamaldehyde treated sample (under MIC) after inoculating a liquid bacterial culture at # of hours time point. The color gradient indicates low to high relative levels of metabolites.

Figure 2. PCA score plot_positive ESI mode: *E.coli* bacteria during growth curve at # hours after bacteria incubation in meida and treatment by cinnamaldehyde above MIC at # hours: CC#, control bacteria during growth curve at # hours after incubation: C#. (Experimental points are related to biological replicates).
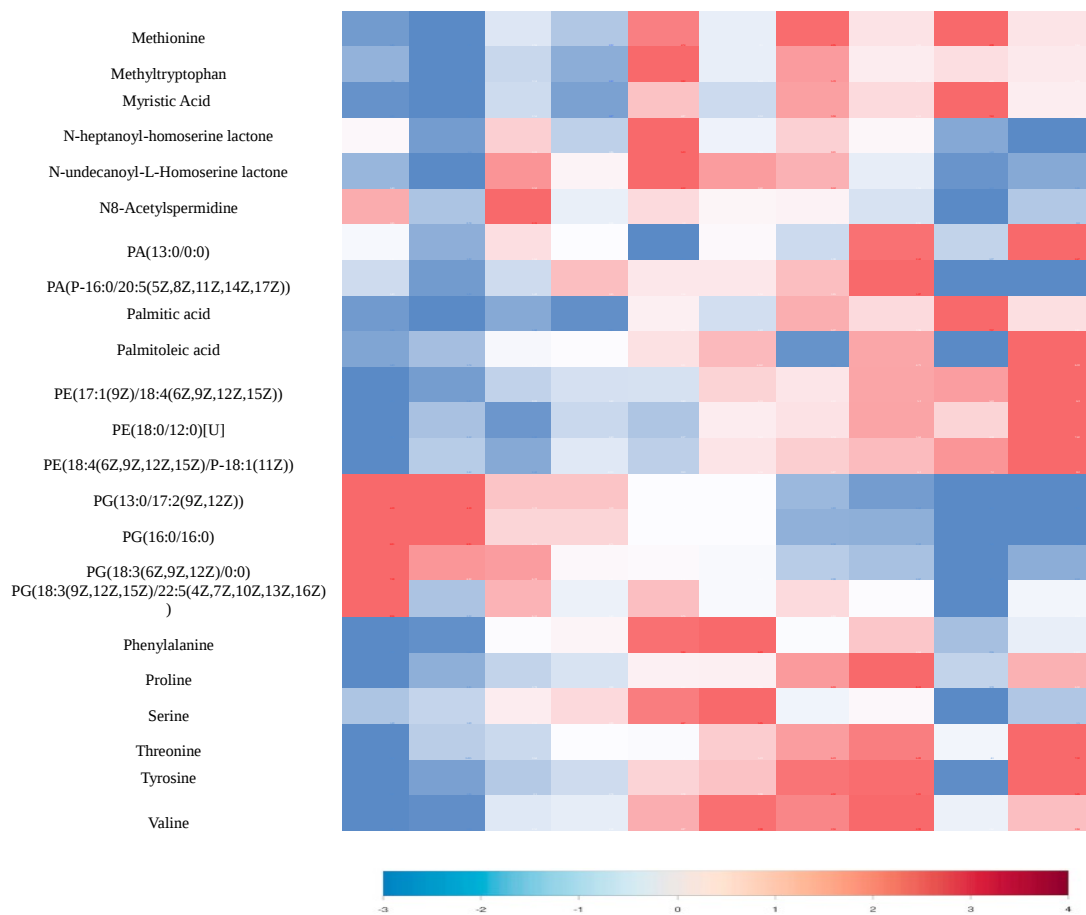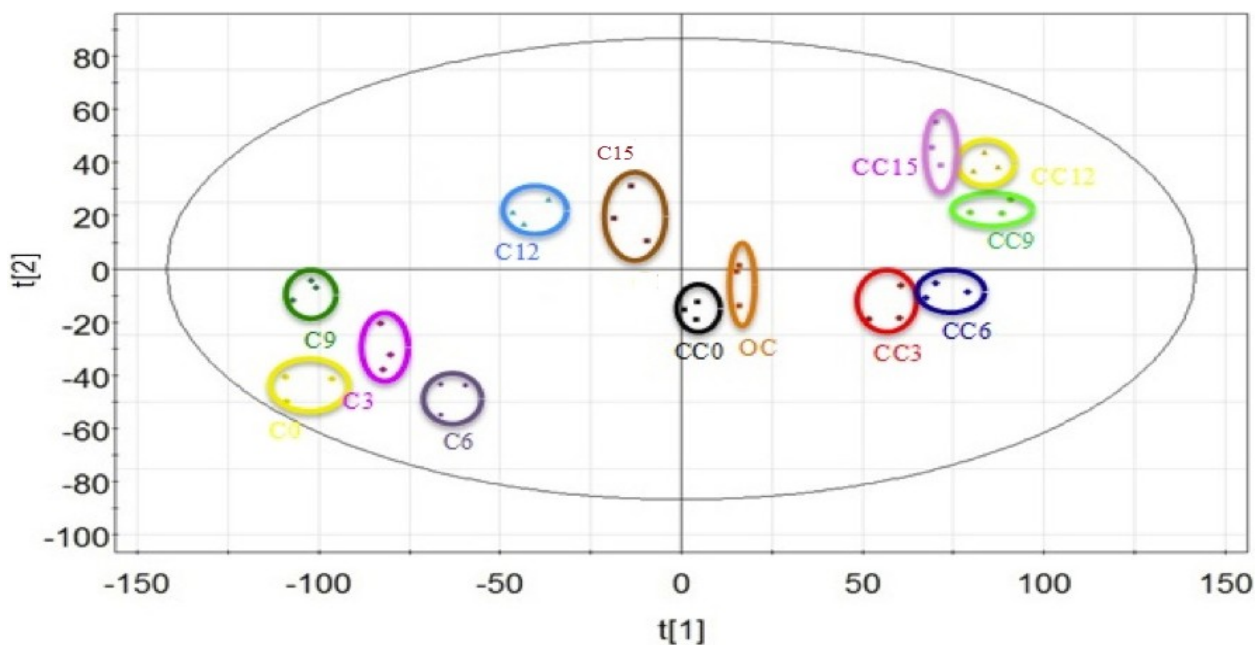
Figure 3. PCA score plot_negative ESI mode: *E.coli* bacteria during growth curve at # hours after bacteria incubation in meida and treatment by CA above MIC at # hours: CC#, control bacteria during growth curve at # hours after incubation: C#. (Experimental points are related to biological replicates).

FIGURES

Figure 1. Heat map of statistically significant metabolic change (p<0.001) between control *E.coli* sample comparison and cinnamaldehyde (under MIC) treated *E.coli* at different time points: #h_C: control sample after inoculation a liquid bacterial culture at # of hours; #h_CA: cinnamaldehyde treated sample (under MIC) after inoculating a liquid bacterial culture at # of hours time point. The color gradient indicates low to high relative levels of metabolites.

Figure 2. PCA score plot_positive ESI mode: *E.coli* bacteria during growth curve at # hours after bacteria incubation in meida and treatment by cinnamaldehyde above MIC at # hours: CC#, control bacteria during growth curve at # hours after incubation: C#. (Experimental points are related to biological replicates).
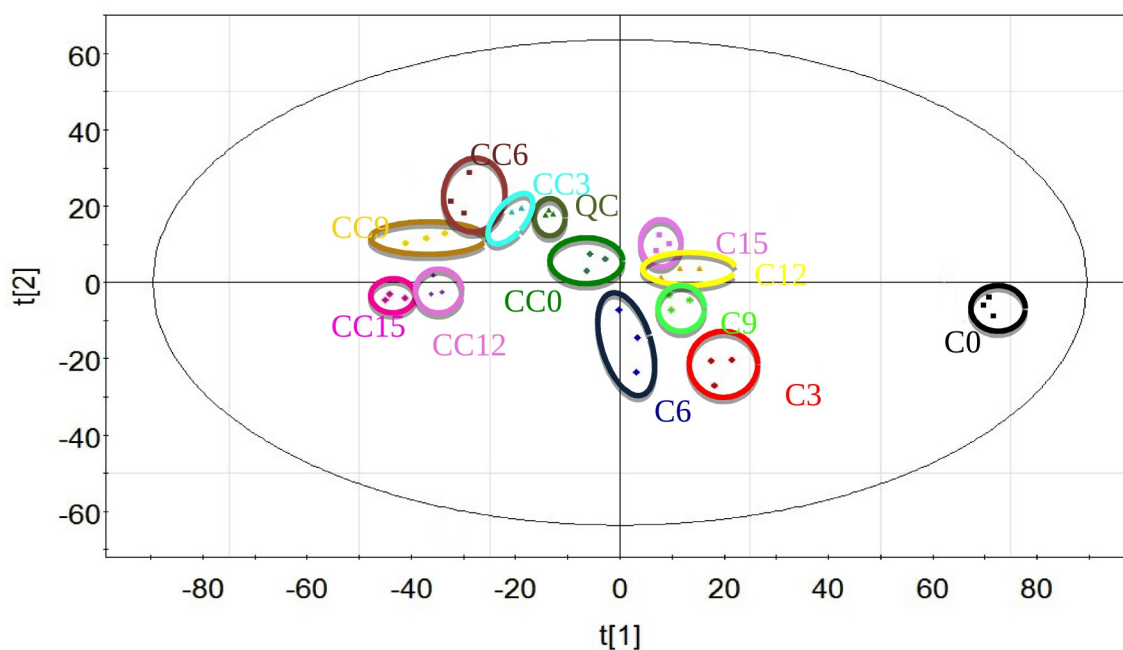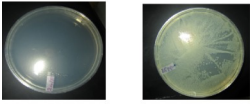

Figure 3. PCA score plot_negative ESI mode: *E.coli* bacteria during growth curve at # hours after bacteria incubation in meida and treatment by CA above MIC at # hours: CC#, control bacteria during growth curve at # hours after incubation: C#. (Experimental points are related to biological replicates)
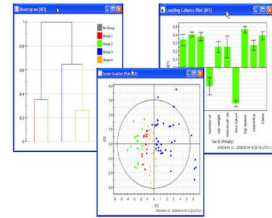
Graphical Abstract

Cinnamaldehyde

Sample preparation (96-blade SPME)

E.coli MIC Identification   LC-MS analysis   Multivariate data analysis